Assignment of the Vibrational Modes of the Chromophores of Iodopsin and Bathoiodopsin: Low-Temperature Fourier Transform Infrared Spectroscopy of ^{13}C- and ^{2}H-Labeled Iodopsins†

Takahiro Hirano,‡,§ Naoko Fujioka,‖ Hiroo Imai,‡,§ Hideki Kandori,§,⊥ Akimori Wada,‖ Masayoshi Ito,‖ and Yoshinori Shichida*,‡,§

Department of Biophysics, Graduate School of Science, Kyoto University, Kyoto 606-8502, Japan, Core Research for Evolutional Science and Technology (CREST), Japan Science and Technology Agency, Japan, Kobe Pharmaceutical University, Kobe 658-8558, Japan, and Department of Materials Science and Engineering, Nagoya Institute of Technology, Showa-ku, Nagoya 466-8555, Japan

Received August 25, 2005; Revised Manuscript Received November 21, 2005

ABSTRACT: To investigate the chromophore structures of iodopsin and its low-temperature photoproducts, we have assigned their vibrational bands in the Fourier transform infrared (FTIR) spectra using iodopsin samples that were reconstituted with a series of ^{13}C- and deuterium-labeled retinals. The analyses of the vibrational bands in the fingerprint and hydrogen-out-of-plane (HOOP) regions indicated that the structure of the chromophores in the iodopsin system differs near their centers from those in the rhodopsin system. Compared to rhodopsin, the chromophore of the batho intermediate of iodopsin is twisted in the C_{12} to C_{14} regions but is more planar around C_{11} region. The large amount of twisting was reduced by removing the chloride ion from the iodopsin, suggesting that this twisting hinders the relaxation of the torsion near C_{11} necessary for the transition to the lumi intermediate and thus results in the thermal reversion of the batho intermediate back to the iodopsin. From the analyses of the C═NH and C═ND stretching bands, we conclude that the displacement of the Schiff base region upon photoisomerization of the chromophore is restricted, as is the case for rhodopsin. These results indicated that iodopsin's chromophore has a unique structure near its center and that this difference is enhanced by the binding of chloride nearby.

Iodopsin (λ_{max} = 571 nm) is a visual pigment present in the chicken red-sensitive cones (*1*) and belongs to a family of long-wavelength-sensitive visual pigments among the four families (short, middle1, middle2, and long, which are abbreviated S, M_1, M_2, and L, respectively) of the cone visual pigments (*2*−*5*). It is different from the cone visual pigments of other families and rod visual pigment rhodopsin in that it has a chloride-binding site in its protein moiety, and binding of the chloride causes a red shift in the absorption maximum (*6*−*9*). The existence of the chloride-binding site is a general feature of pigments belonging to group L (*10*, *11*) except in rodents (*12*−*16*). The chloride-binding site also accommodates various monovalent anions, but most anions except for halides induce only small shifts (*9*, *10*) of the absorption maximum. Studies using nitrate as the substituting anion showed that it can bind to the same binding site competitively with chloride but it blue shifts the absorption maximum about 40 nm compared to the chloride-bound form (*17*). In addition, chloride binding also controls the thermal behavior of bathoiodopsin produced at liquid nitrogen temperature (−196 °C): bathoiodopsin produced from chloride-bound iodopsin at −196 °C thermally reverts to the original iodopsin, while bathoiodopsin produced from nitrate-bound iodopsin decays to lumiiodopsin as bathorhodopsin produced from rhodopsin does (*17*−*20*). Thus, it is of interest to investigate how the chloride binding affects the structure and the electronic state of the chromophore of iodopsin and bathoiodopsin.

In our previous studies, we have investigated the effect of anions on the absorption maximum by comparing the low-temperature FTIR[1] spectra of the chloride- and nitrate-bound forms and the anion-unbound form of iodopsin (iodopsin·Cl, iodopsin·NO_3, and iodopsin·free, respectively) (*21*, *22*). Comparison of these spectra revealed that several chromophore vibrational bands such as C−C stretching (fingerprint region), hydrogen-out-of-plane (HOOP) wagging, and C═NH (and C═ND) stretching modes were identical or quite similar among the three species; an exception was the ethylenic vibrations. The vibrational bands of the pigments' amide bonds also showed similarities. On the other hand, the bands of the batho state for iodopsin·free were similar to those for iodopsin·NO_3 but considerably different from

† This work was supported in part by Grants-in-Aid for Priority Areas and the Grant for Biodiversity Research of the 21st Century COE (A14) from the Japanese Ministry of Education, Culture, Sports, Science, and Technology to Y.S.

* To whom correspondence should be addressed. Phone: +81-75-753-4213. Fax: +81-75-753-4210. E-mail: shichida@vision-kyoto-u.jp.

‡ Kyoto University.

§ CREST.

‖ Kobe Pharmaceutical University.

⊥ Nagoya Institute of Technology.

[1] Abbreviations: FTIR, Fourier transform infrared; HEPES, *N*-(2-hydroxyethyl)piperazine-*N*′-2-ethanesulfonic acid; CHAPS, 3-[(3-cholamidopropyl)dimethylammonio]-1-propanesulfonate; PC, L-α-phosphatidylcholine from egg yolk; CHAPS/PC, buffer solution that contains a mixture of CHAPS and PC; Con A, concanavalin A; DTT, dithiothreitol; PMSF, phenylmethanesulfonyl fluoride; KIU, kallikrein inhibitor units.

10.1021/bi0517077 CCC: $33.50
Published on Web 01/06/2006

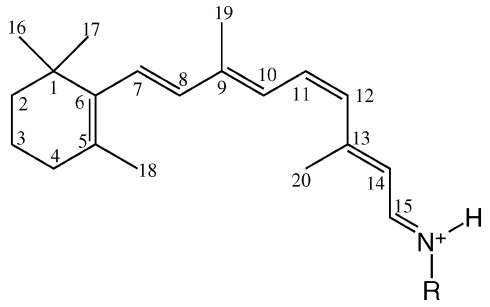

FIGURE 1: Structural formula for retinal protonated Schiff base (PSB) in the 11-cis form. "R" represents the protein moiety including the lysine residue (Lys296 in bovine rhodopsin; Lys309 in iodopsin) that forms a covalent bond with the chromophore.

those for iodopsin·Cl. These results suggested that the binding of chloride but not nitrate induces a conformational change in the protein and that the chloride-binding site is situated at a position where it directly interacts with the chromophore when the chromophore is photoisomerized.

FTIR studies of the three types of iodopsin samples gave valuable information about anion binding, but difficulties still remain in describing the mechanism of anion binding. In our previous studies (*21*, *22*), we assigned the FTIR bands by analogy with the results for the resonance Raman spectra of bovine rhodopsin (*23*), but the validity of the band assignment needed to be strengthened. In the present study, in order to assign each band in the FTIR difference spectra of iodopsin, the FTIR spectra of iodopsin samples that are regenerated with the ^{13}C- and ^{2}H (D)-substituted retinal derivatives (Figure 1) were measured. From this data, each band in the FTIR spectra is assigned to a specific vibrational mode of the chromophore in the HOOP, fingerprint, and C═N stretching regions. On the basis of the assignment, we will discuss the chloride effect on the chromophore structure of iodopsin and bathoiodopsin. We will also consider how chloride binding induces the thermal reversion of bathoiodopsin back to iodopsin.

MATERIALS AND METHODS

Synthesis of D- and ^{13}C-Labeled Retinal Derivatives. *all-trans*-D-labeled retinals were synthesized according to previously reported methods (*24*−*26*). 11-Cis isomers were separated by HPLC from the photoisomerized mixtures of the corresponding *all-trans*-retinals, respectively. Five ^{13}C-labeled retinals (the labeled position is indicated in brackets) were prepared from β-ionone-tricarbonyliron complexes according to the previously reported methods (*27*) in which the labeled reagents such as acetonitrile-2-^{13}C [10], acetonitrile-1-^{13}C [11], ethyl trimethylsilylacetate-2-^{13}C [12], ethyl trimethylsilylacetate-1-^{13}C [13], and methyl-^{13}C-magnesium iodide [20] were used. The Peterson reactions of C-18-ketone-tricarbonyliron complexes with ethyl trimethylsilylacetate-2-^{13}C [14] and ethyl trimethylsilylacetate-1-^{13}C [15] afforded the corresponding labeled ethyl retinoate-tricarbonyliron complexes, which were converted to the 14 and 15 labeled 11-*cis*-retinals by successive sequences of decomplexation of the tricarbonyliron, reduction of the ester, and MnO_2 oxidation.

7-^{13}C, 8-^{13}C, and 9-^{13}C labeled β-ionones were prepared as reported by Lugtenburg (*28*). 19-^{13}C labeled β-ionone was produced by the reaction of *N*-methoxy-*N*-methyl-3-(2,6,6-trimethyl-1-cyclohexen-1-yl)-2-propenamide with methyl-^{13}C-magnesium iodide. These four labeled β-ionones were converted to the tricarbonyliron complexes, and then transformed into the corresponding labeled 11-*cis*-retinals as described in the literature (*27*).

Iodopsin Sample Preparation. The iodopsin samples for FTIR measurements were prepared as previously described (*21*, *22*). Briefly, iodopsin was extracted from about 2000 chicken retinas by a mixture of CHAPS and PC. The crude iodopsin sample was purified by Con A-Sepharose affinity and SP-Sepharose ion exchange columns (Pharmacia) and then adsorbed again on a Con A-Sepharose column equilibrated with buffer A [20% glycerol (w/v), 0.6% CHAPS, 0.8 mg/mL PC, 50 mM HEPES, 140 mM NaCl, 1 mM DTT, 0.1 mM PMSF, 4 μg/mL leupeptin, and 50 KIU/mL aprotinin, pH 6.6] supplemented with 1 mM $MnCl_2$ and $CaCl_2$. After the column was washed with buffer A supplemented with 1.5 mM methyl α-D-mannoside to remove the other contaminating pigments, iodopsin was eluted with buffer A supplemented with 200 mM methyl α-D-mannoside (*29*). In order to prepare an iodopsin sample with a ^{13}C-labeled chromophore, the purified iodopsin was photobleached at 4 °C, followed by adding an equivalent molar amount of each ^{13}C-labeled retinal solubilized in ethanol. The regeneration reaction of the pigment was monitored by a UV−vis spectrophotometer. Excess retinal was converted to retinal oxime by adding NH_2OH to a final concentration 10 mM. Each sample was then dialyzed against buffer C [50 mM HEPES, 140 mM NaCl, 1 mM DTT, 0.1 mM PMSF, 4 μg/mL leupeptin, and 50 KIU/mL aprotinin, pH 6.6] to prepare the PC liposome containing iodopsin. After 1 h dialysis, buffer C was exchanged with new one. This procedure was repeated three times. Then buffer C was exchanged after dialysis for 3 h and the exchange procedure was repeated two more times. The resulting sample was centrifuged, and the pellet was suspended in 10 mM NaCl solution.

A drop of the PC liposome suspension was then applied to a BaF_2 window (18 mm, OYO-KOKEN), followed by drying at 4 °C overnight. About 1 μL of either H_2O or D_2O was placed beside the film for humidification, and the unit was sealed with another BaF_2 window with the aid of a silicone rubber O-ring and placed in a brass cell holder. The extent of the sample hydration was monitored by the absorbance of the O−H (or O−D) stretching region in the IR absorption spectrum.

Spectrophotometry. UV−vis absorption spectra were recorded with a Shimadzu model MPS-2000 spectrophotometer interfaced with an NEC PC-9801 computer. The system for recording the absorption spectra was reported previously (*21*, *22*, *29*). FTIR spectra were recorded by a Bio-Rad FTS-60A/896 spectrometer according to methods described previously (*21*, *22*, *30*). An Oxford model DN-1704 cryostat was used for cooling the sample. The temperature of the sample was regulated to within 0.1 °C with a temperature controller (ITC-4, Oxford). The sample was irradiated with light from a 1-kW tungsten halogen lamp (Rikagaku Seiki) which had been passed through a glass cutoff filter (VR68, VR63; Toshiba) or an interference filter (501 nm, Nihonshinku; and 700 nm, Toshiba). The conditions of irradiation to obtain the difference FTIR spectra of all the labeled iodopsin samples were identical with those reported previously for

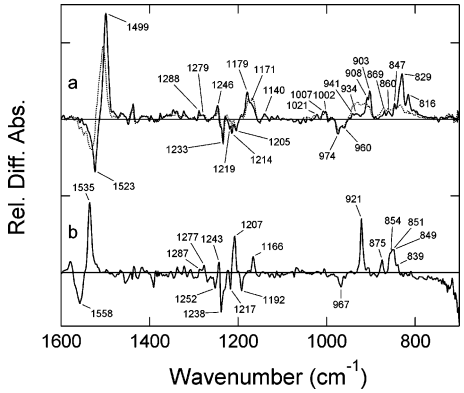

FIGURE 2: FTIR difference spectra of batho/iod (a) and batho/rh (b) in the 1600−700 cm^{-1} region. Corresponding difference spectrum of the anion-free iodopsin sample is superimposed on the upper curve (dotted line). Each spectrum was recorded at −196 °C. These data were taken from papers published previously (*21*, *22*, *30*).

iodopsin·Cl (*21*, *22*). For each measurement, 128 interferograms were accumulated. The difference FTIR spectra shown in the figures are the averages of 8−16 measurements.

RESULTS

Comparison between FTIR Spectra of Iodopsin and Rhodopsin. Figure 2 shows the batho/original FTIR difference spectra in the 1600−800 cm^{-1} region of iodopsin (panel a, solid line, chloride-bound; dotted line, anion-free) (*21*, *22*) and bovine rhodopsin (panel b) (*30*). The FTIR spectrum of iodopsin basically retains the features of the rhodopsin spectrum, but significant differences are observed according to the structural differences among their chromophore and protein moieties. A triplet feature appears in the iodopsin side at 1219, 1214, and 1205 cm^{-1} but cannot be observed in the rhodopsin spectrum. The vibrational mode that appears as the 1166 cm^{-1} peak in bathorhodopsin is observed as doublet peaks at 1179 and 1171 cm^{-1} in bathoiodopsin. The HC_{11}═$C_{12}H$ HOOP band of rhodopsin appears at 967 cm^{-1}, while iodopsin has two peaks at 974 and 960 cm^{-1} in the corresponding locus. Spectral differences are more obvious on the batho side. The 11-HOOP band of bathorhodopsin appears at 921 cm^{-1}. Bathoiodopsin has two peaks at 908 and 903 cm^{-1}, one or both of which could be assumed to correspond to the 11-HOOP mode. The 829 cm^{-1} peak is the most intense band of bathoiodopsin in the HOOP region, while only rather small peaks are present in bathorhodopsin in that locus. This 829 cm^{-1} band decreases its intensity upon the removal of chloride bound to the iodopsin pigment or an exchange of chloride for nitrate. In addition, the small bands at 934 and 941 cm^{-1} increase in intensity upon the removal of chloride (Figure 2, dotted line). In order to assign the vibrational bands of the chromophore that appear in the 1800−800 cm^{-1} region of the FTIR spectra of iodopsin, the FTIR spectra of iodopsin samples which have systematically isotopic labeled retinal as their chromophore were measured. The results are shown for four specific frequency regions of the FTIR spectra of the three isomeric forms, iodopsin, bathoiodopsin, and isoiodopsin.

Ethylenic Stretching Modes. Figure 3 shows the batho/iod and batho/iso FTIR difference spectra of iodopsin samples with ^{13}C-labeled retinal chromophores in the 1600−1400 cm^{-1} region. It is well-known that the ethylenic

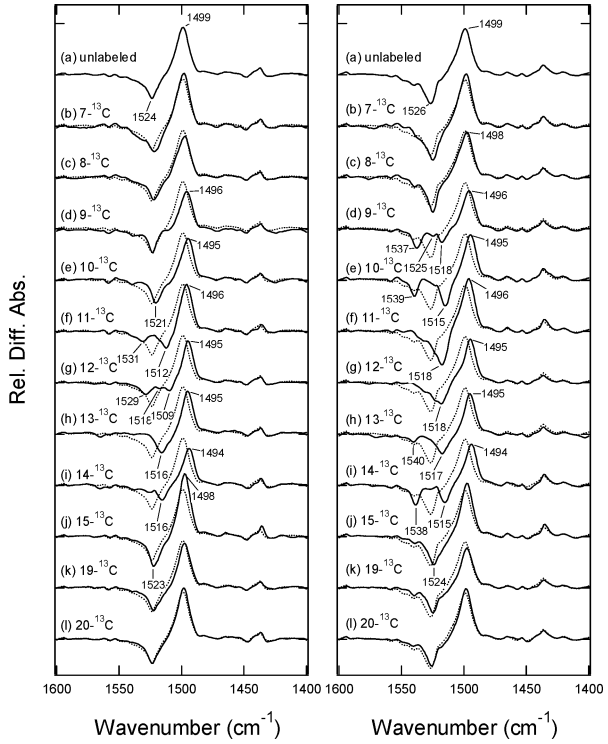

FIGURE 3: FTIR difference spectra of (a) unlabeled and (b) 7-^{13}C-, (c) 8-^{13}C-, (d) 9-^{13}C-, (e) 10-^{13}C-, (f) 11-^{13}C-, (g) 12-^{13}C-, (h) 13-^{13}C-, (i) 14-^{13}C-, (j) 15-^{13}C-, (k) 19-^{13}C-, and (l) 20-^{13}C-labeled iodopsin in the 1600−1400 cm^{-1} region. Difference spectra of batho/iod (left panel) and batho/iso (right panel) are presented with the spectrum of an unlabeled iodopsin sample superimposed (dotted lines).

stretching modes (C═C stretching modes) of the chromophore are observed in this area. The C═C stretching modes of iodopsin, bathoiodopsin, and isoiodopsin are respectively observed at 1524, 1499, and 1526 cm^{-1} in the difference spectra. The ethylenic band of iodopsin shows a slight downshift to 1521 cm^{-1} when the C_{10} carbon of the chromophore is labeled. A rather larger downshift to 1516 cm^{-1} is observed when the C_{13} or C_{14} carbon is labeled. In the case of an 11-^{13}C-labeled sample, this band splits in two peaks at 1531 and 1512 cm^{-1}. Similarly when the C_{12} carbon is labeled, the band splits into two peaks at 1529 and 1509 cm^{-1}. This trend suggests that this ethylenic mode includes the displacements of C_{10} to C_{14} carbons, and especially those of the C_{11} and C_{12} positions make a large contribution to this vibrational mode. On the other hand, the corresponding band of bathoiodopsin shows only slight downshifts of 3−5 cm^{-1} for almost all spectra of ^{13}C-labeled iodopsin; otherwise no change was observed. This result suggests that this vibrational mode of bathoiodopsin is not a localized one, but instead quite delocalized. In the case of isoiodopsin, the band split is observed when the C_9, C_{10}, C_{14} position is labeled. In addition, a large downshift is observed when the C_{11} to C_{13} position is labeled.

HOOP Modes. Figures 4 and 5 show the FTIR difference spectra of iodopsin samples with ^{13}C- and D-labeled retinal chromophores in the 1100−800 cm^{-1} region, respectively. Batho/iod and batho/iso difference spectra are shown in both figures. In this area, the hydrogen-out-of-plane (HOOP) vibrational bands of the chromophore are observed. The 974 and 960 cm^{-1} bands of iodopsin slightly downshift upon labeling at C_{11} and C_{12} (Figure 4, left panel). This result is

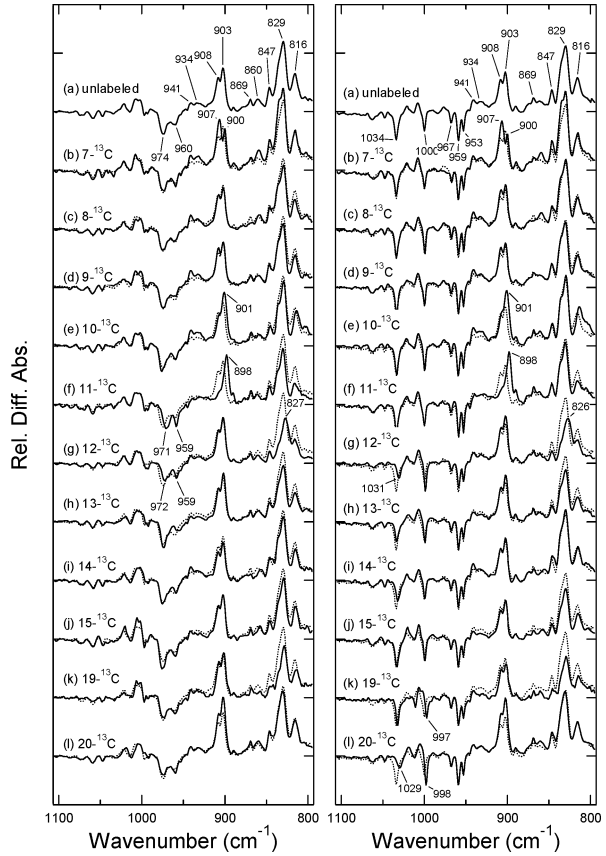

FIGURE 4: Batho/iod (left panel) and batho/iso (right panel) FTIR difference spectra of (a) unlabeled and (b) 7-^{13}C-, (c) 8-^{13}C-, (d) 9-^{13}C-, (e) 10-^{13}C-, (f) 11-^{13}C-, (g) 12-^{13}C-, (h) 13-^{13}C-, (i) 14-^{13}C-, (j) 15-^{13}C-, (k) 19-^{13}C-, and (l) 20-^{13}C-labeled iodopsin samples in the 1100−800 cm^{-1} region. Dotted lines are the spectra of an unlabeled iodopsin sample.

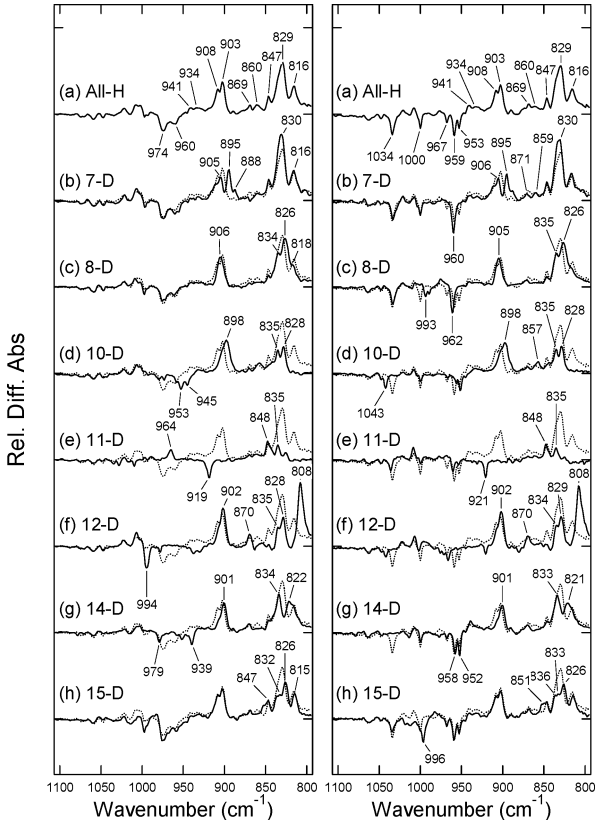

FIGURE 5: Batho/iod (left panel) and batho/iso (right panel) FTIR difference spectra of (a) unlabeled and (b) 7-D-, (c) 8-D-, (d) 10-D-, (e) 11-D-, (f) 12-D-, (g) 14-D-, and (h) 15-D-labeled iodopsin samples in the 1100−800 cm^{-1} region. Spectra were measured in the same way as the ^{13}C-labeled iodopsin. Dotted lines are the spectra of an unlabeled iodopsin sample. The data for 8-D- and 14-D-labeled batho/iod spectra have been reported previously (*22*).

reasonable because these bands are assumed from the spectral similarity to correspond to the 967 cm^{-1} HC_{11}═$C_{12}H$ HOOP band of rhodopsin, as shown in Figure 2. The 960 cm^{-1} band also shifts upon labeling at the C_{13} position, decreasing its intensity, suggesting that this band also includes displacement of the C_{13} carbon of the chromophore, while the 974 cm^{-1} band does not shift. These bands are affected by D labeling of the carbon atoms from 10 to 14 positions (Figure 5). These bands showed no shift upon ^{13}C or D labeling at other positions of the retinal, indicating that these vibrational modes come exclusively from the 11 to 14 area of the chromophore. In the 11-D and 12-D labeled spectra, residual negative bands exist at 919 and 994 cm^{-1}, respectively. The negative band at 994 cm^{-1} is also observed in the 11,12-D_2-labeled spectrum (data not shown). Thus, this band could be assigned to some vibrational mode that couples with the 12-H wagging mode of iodopsin, which is most likely to be the 13-methyl rocking vibration.

For the batho side, at least five bands are observed at 908, 903, 847, 829, and 816 cm^{-1} in addition to small bands at 869 and 860 cm^{-1}. Among these, three bands showed obvious downshifts upon ^{13}C labeling of a certain position of the chromophore. The doublet band at 908 and 903 cm^{-1} shifts to 898 cm^{-1} upon isotope labeling at C_{11}, losing its doublet nature. The 908 and/or 903 cm^{-1} bands are also slightly affected by labeling at C_7 and C_{10}, suggesting that these modes weakly couple with some modes including the displacement of C_7 and C_{10} of the chromophore. It should be noted that these bands did not show any change upon labeling at C_{12}. These bands vanish (shift to a lower frequency region) on D labeling of 11-H, supporting the assignment that these bands are from the 11-HOOP mode of the chromophore. The 908 cm^{-1} band also vanished on isotope labeling at 10-H and 14-H, where the effect of 14-D labeling is somewhat clearer. This doublet band is also affected by labeling at 7- and 8-H. The 829 cm^{-1} band of bathoiodopsin showed a slight shift upon labeling at C_{12} with a large decrease in its intensity. A decrease in the intensity of this band was also observed with labeling at C_{19} (carbon of the 9-methyl group). Isotope labeling of 11-H largely decreases the intensity of this band, indicating that this band also contains displacement of 11-H though that of C_{11} is not included. This band is also affected by D labeling at 10, 12, 14, and 15. The remaining peak around 829 cm^{-1} is observed in D labeling at positions other than 14-H. Thus, the 829 cm^{-1} band is mainly attributed to the 14-H and 12-H wagging modes, though it significantly contains other wagging modes.

The 816 cm^{-1} band completely goes out of the frequency region by 10- and 11-D labeling and is significantly affected by 8- and 12-D and 10-^{13}C labeling. Thus, this band could be assigned to the 10-HOOP mode, though it contains other vibrational modes. The 847 cm^{-1} band changes its shape upon 19-^{13}C labeling. It seems to be affected by ^{13}C labeling at other positions, though it is difficult to evaluate the effect of each labeling because of the low band intensity. This band is also affected by both 10- and 12-D labeling, but the effect

seems much larger for 12-D labeling. Thus, this mode could be assigned to the 12-HOOP mode coupled with the 10-H wagging and 13-methyl rocking modes. The 869 cm^{-1} band seems to be affected by 8-^{13}C and 7-, 8-, and 11-D labeling that could be assigned to the $HC_7{=}C_8H$ HOOP mode. The 860 cm^{-1} band is slightly affected by 13-^{13}C labeling and by D labeling at 8-, 12-, 14-, and 15-H. It also seems to shift slightly upon labeling at C_{14} and C_{15}. Thus, this mode could be assigned to a coupled mode that mainly contains 14-H and 15-H wagging modes.

The 829 cm^{-1} band is expected to have a shoulder band in its higher frequency end (~835 cm^{-1}). Because the intensity at this frequency always remains for any position of isotope labeling, this band should originate from the β-ionone part of the chromophore or from the protein moiety. This band also remains when the chloride bound to iodopsin is replaced by nitrate or is removed (*21*, *22*). In addition to these bands, small peaks are observed at 941 and 934 cm^{-1}. These bands largely increase their intensity upon removal of chloride (Figure 2) (*21*). Both of these bands disappear upon 11-D and 12-D labeling. They also seem to slightly downshift upon labeling at C_{11}. Thus, these bands are assigned to the coupled $HC_{11}{=}C_{12}H$ wagging mode.

Five large peaks appear in this region for isoiodopsin (Figure 4, right panel). The triplet band at 967, 959, and 953 cm^{-1} showed no change upon labeling at any position of the carbon atom. This result indicates that these modes do not contain displacements of C_7 to C_{15} atoms of the chromophore. The band at 967 cm^{-1} is affected by labeling of the hydrogen atoms at positions 7, 8, and 11, while the 953 cm^{-1} band is affected by labeling at positions 7, 8, 11, and 12. The 959 cm^{-1} band is affected by labeling at 10, 11, and 12. These results indicate that this triplet band contains displacements of hydrogen at the 7, 8, 11, and 12 positions, namely, the $HC_7{=}C_8H$, 11-H, and 12-H wagging modes, and are differently mixed. The 1034 cm^{-1} band shifts upon labeling at C_{12} and C_{20}. Deuterium labeling at 10, 12 and 14 positions also affects this band, and the effect of 14-D labeling is the most obvious among them. Thus, this mode was assigned to a coupling mode of 12-, 14-H wagging and 13-methyl rocking vibrational modes. The 1000 cm^{-1} band is affected by labeling at C_{19} and C_{20}. This band also looks affected by D labeling at 8, 10, 11, and 12, though the effects other than 8-D labeling are not so clear. Thus, this band was assigned to a coupling mode of 8-H wagging and the 9-methyl rocking vibrational modes.

Fingerprint Region. Figure 6 shows batho/iod and batho/iso FTIR difference spectra of iodopsin samples with ^{13}C-labeled retinal chromophores in the 1300−1100 cm^{-1} region. In this area, fingerprint vibrational bands (C−C stretching modes) of the chromophore are mainly observed. For the iodopsin side in the unlabeled batho/iod difference spectrum, at least four bands can be observed at 1233, 1219, 1214, and 1205 cm^{-1} (Figure 6, left panel). The 1205 cm^{-1} band is affected by labeling at C_{10} to C_{13}. However, it more obviously shifts downward by labeling at C_{14} and C_{15} to 1195 and 1198 cm^{-1}, respectively. This result clearly shows that the 1205 cm^{-1} band mainly comes from the $C_{14}{-}C_{15}$ stretching mode, though it also contains the $C_{12}{-}C_{13}$ stretching mode to some extent. The largest 1233 cm^{-1} band is affected by isotope labeling of the carbons at positions from C_{13} to C_{15} with a slight downshift and decrease in intensity

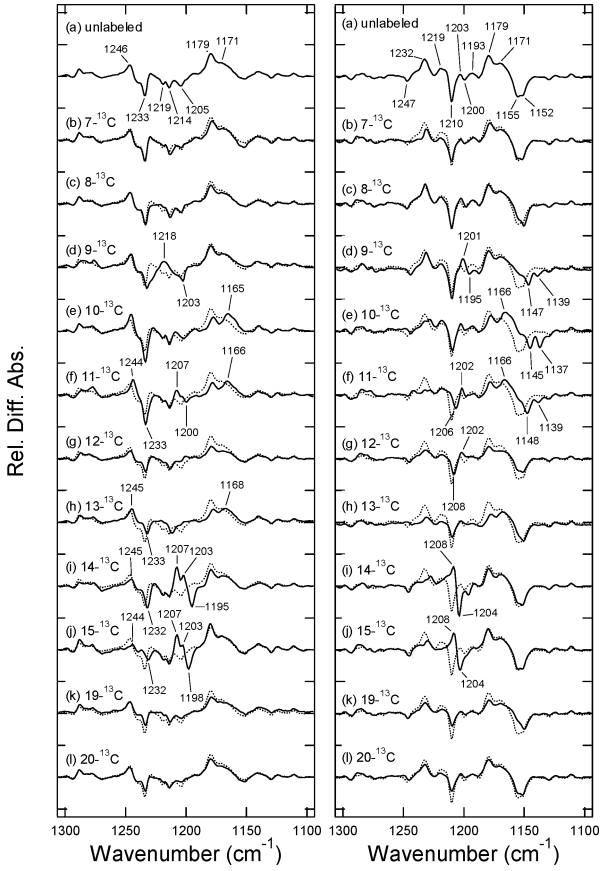

FIGURE 6: Batho/iod (left panel) and batho/iso (right panel) FTIR difference spectra of (a) unlabeled and (b) 7-^{13}C-, (c) 8-^{13}C-, (d) 9-^{13}C-, (e) 10-^{13}C-, (f) 11-^{13}C-, (g) 12-^{13}C-, (h) 13-^{13}C-, (i) 14-^{13}C-, (j) 15-^{13}C-, (k) 19-^{13}C-, and (l) 20-^{13}C-labeled iodopsin samples in the 1300−1100 cm^{-1} region. Dotted lines are the spectra of an unlabeled iodopsin sample.

but is little affected by labeling at C_{12}. The 1219 cm^{-1} band vanishes or shifts downward by labeling at the C_8, C_9, C_{12}, C_{13}, and C_{19} (9-methyl) positions. This result suggests that this band consists of the $C_8{-}C_9$, $C_{12}{-}C_{13}$ stretching modes and the 9-methyl rocking mode. The 1214 cm^{-1} band vanishes on labeling at C_9 and is slightly affected by labeling at C_{13}. Thus, it is difficult to assign these bands to some specific C−C stretching modes.

For the batho side of the batho/iod and batho/iso difference spectra, four obvious peaks can be observed at 1246, 1232, 1179, and 1171 cm^{-1}. Three small bands can also be observed at 1219, 1203, and 1193 cm^{-1} in the batho/iso spectrum. The highest band at 1246 cm^{-1} is affected by labeling at C_{15}. This band is slightly affected by labeling at the C_{11}, C_{13}, and C_{14} positions. Thus, this band could not be assigned to certain localized vibrational mode. The lowest band in this region at 1171 cm^{-1} shows a downshift or decrease in intensity by labeling at C_{10} to C_{13}, though the effect of labeling at C_{12} is not clear compared to other position labeling. Thus, this 1171 cm^{-1} peak is assigned to the $C_{10}{-}C_{11}$ stretching mode. In addition, the 1230 to 1220 cm^{-1} region of the batho/iod difference spectrum is, though there are no clear batho peaks, somewhat affected by labeling at C_9 of the chromophore. Because only a slight change occurs in that region of the C_9-labeled batho/iso spectrum (Figure 6, right panel), the large spectral change in the batho/iod spectrum upon C_9 labeling comes from a vibrational

mode of the iodopsin side, though it cannot be assigned to a particular peak in the difference spectrum. In fact, a similar spectral change in this region is observed in the iso/iod difference spectrum upon C_9 labeling (data not shown).

For the batho side of the batho/iso difference spectra, the small peak at 1219 cm^{-1} shifts to 1208 cm^{-1} upon labeling at C_{14} ant C_{15}. These results clearly show that this band represents the $C_{14}-C_{15}$ stretching mode of the bathoiodopsin chromophore. The 1203 cm^{-1} band appears affected by labeling at C_9, C_{11}, C_{14}, and C_{15}, though the effect of labeling at C_{14} and C_{15} is not clear because the negative band (iso side) at 1204 cm^{-1} affects the band shape of the positive 1203 cm^{-1} band. Thus, the candidate for this band is the C_8-C_9 stretching mode. The 1193 cm^{-1} band decreases in intensity on labeling at C_{13}. This band appears affected by other positions of the chromophore, but it is difficult to evaluate the contribution of each carbon atom mode because of its small and broad band shape. The 1232 cm^{-1} band is affected by labeling at almost all the carbon atoms in the polyene region. Thus, this band would arise from a global vibration of the polyene chain.

Isoiodopsin has four major bands in this region at 1247, 1210, 1155, and 1152 cm^{-1} (Figure 6, right panel). A small band at 1200 cm^{-1} is also observed. The 1247 cm^{-1} band shows slight shifts upon labeling from C_9 to C_{15}, indicating that this band does not come from a vibrational mode localized in a certain part of the chromophore. The sharp band at 1210 cm^{-1} shows clear downshifts to 1204 and 1203 cm^{-1} on labeling at C_{14} and C_{15}, respectively. Although some other parts of the chromophore have a slight effect on this band, it can be assigned to the $C_{14}-C_{15}$ stretching mode of the isoiodopsin chromophore. The lowest doublet band at 1155 and 1152 cm^{-1} shows clear downshifts by labeling at C_9 to C_{11}, with its doublet nature becoming clearer. The 1155 cm^{-1} band is also affected by labeling at C_{13} and C_{19}. Thus, the band at 1152 cm^{-1} is assumed to consist mainly of $C_{10}-C_{11}$ stretching mode, and that at 1155 cm^{-1} is mainly $C_{10}-C_{11}$ stretching mode and the 9-methyl rocking mode. The small band at 1200 cm^{-1} shows a clear downshift to 1195 cm^{-1} upon labeling at C_9. This band is also affected by labeling from C_{12} to C_{15}. Thus, though it is difficult to assign this band to a specific C−C stretching mode, it could be assigned to a vibrational mode that mainly contains the C_8-C_9 stretching mode. Difference spectra of D-labeled iodopsin in the fingerprint region are so complicated that no attempt was made to derive any supporting information for assignment of C−C stretching vibrations (data not shown).

C═N Stretching Mode of the Protonated Schiff Base. The left panel of Figure 7 shows the FTIR difference spectra of 15-^{13}C, 15-D iodopsin, and D_2O-humidified iodopsin samples in the 1750−1550 cm^{-1} region. In this region, the C═N stretching mode of the protonated Schiff base is observed that is formed with the chromophore and the Lys residue on TM7. The C═N stretching mode is known to couple with N−H in the plane rocking mode (C═NH stretching mode), thus this mode is sensitive to the environment around the PSB (*32*). This property is readily confirmed by replacing the proton bound to the nitrogen with deuterium by humidifying the sample with D_2O. The difference in frequency between C═NH and C═ND stretching modes represents a good measure of the strength of hydrogen bonding of the N−H bond (*32*, *33*). In the case of the iso/iod difference

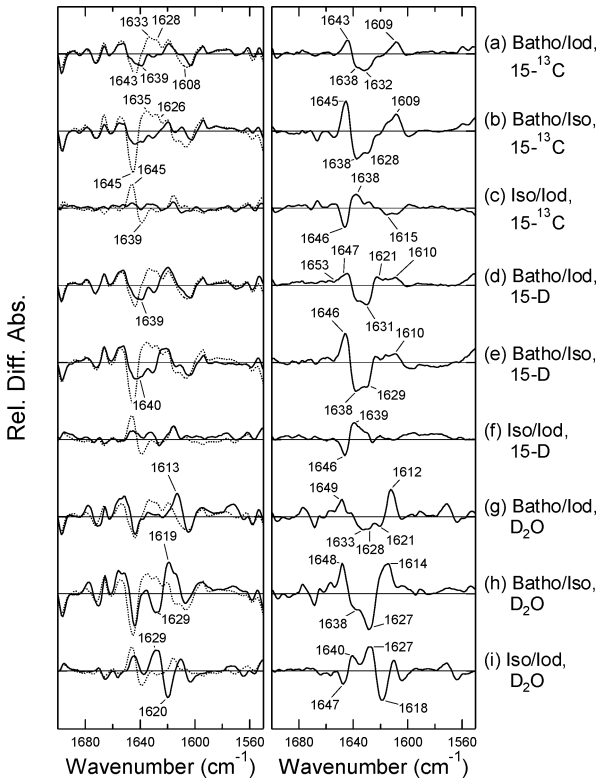

FIGURE 7: FTIR difference spectra (left panel) and their corresponding labeled *minus* unlabeled double difference spectra (right panel) of (a) 15-^{13}C-labeled batho/iod, (b) 15-^{13}C-labeled batho/iso, (c) 15-^{13}C-labeled iso/iod, (d) 15-D-labeled batho/iod, (e) 15-D-labeled batho/iso, (f) 15-D-labeled iso/iod, (g) unlabeled batho/iod in D_2O, (h) unlabeled batho/iso in D_2O, and (i) unlabeled iso/iod in D_2O in the 1750−1550 cm^{-1} region. Dotted lines in the left panel are the spectra of an unlabeled iodopsin sample in H_2O. The difference and double difference spectra for batho/iso and iso/iod in D_2O have been reported previously (*22*).

spectrum, the bilobic band at 1645/1639 cm^{-1} shows a downshift to 1629/1620 cm^{-1} upon deuteration (Figure 7, curve i in the left panel) (*22*). The labeled (D_2O) *minus* unlabeled (H_2O) double difference spectrum (right panel of Figure 7, curve i) exhibits two bilobic bands, 1640/1647 cm^{-1} and 1627/1618 cm^{-1}. Thus, these bands at 1640 and 1647 cm^{-1} are assigned to the C═NH stretching mode of iodopsin and isoiodopsin, respectively. Simultaneously, the 1627 and 1618 cm^{-1} bands are assigned to the C═ND stretching modes of isoiodopsin and iodopsin, respectively. Similarly, the C═NH and C═ND stretching modes of bathoiodopsin could be attributed to 1638 and 1614 cm^{-1}, respectively, from the corresponding double difference spectrum of batho/iso (right panel of Figure 7, curve h). These assignments should be directly confirmed by the spectrum of the 15-^{13}C-labeled samples. In fact, these bands shift upon ^{13}C labeling at C_{15} of the chromophore (Figure 7, curves a−c). In addition, these bands are affected by D labeling at C_{15}-H (Figure 7, curves d−f). The C_{15}-H in-plane rocking mode is known to couple with the C═NH stretching vibration of the PSB (*34*−*37*). Though the existence of shifted bands is only implied in the double difference spectra for both cases, these results together strongly support the assignment of the C═NH stretching modes which we previously presented on the basis of D_2O substitution (*22*).

Table 1: Band Assignments for the FTIR Difference Spectra of Iodopsin and Its Photoproducts[a]

product	frequency (cm^{-1})	assignment
iod	960	HC_{11}═$C_{12}H$ wag, 13-Me rock
	974	HC_{11}═$C_{12}H$ wag
	1205	C_{14}−C_{15} str, C_{12}−C_{13} str
	1214	nd
	1219	C_8−C_9 str, C_{12}−C_{13} str
	1233	nl
	1640	C═NH str (C═ND str: 1618)
batho	816	10-H wag
	829	12-H + 14-H wag
	847	12-H wag
	860	14-H + 15-H wag
	869	HC_7═C_8H wag
	903	11-H wag
	908	11-H + 14-H wag
	934	HC_{11}═$C_{12}H$ wag
	941	HC_{11}═$C_{12}H$ wag
	1171	C_{10}−C_{11} str
	1179	nd
	1193	nd
	1203	C_8−C_9 str
	1219	C_{14}−C_{15} str
	1232	nl
	1246	nl
	1638	C═NH str (C═ND str: 1614)
iso	953	HC_7═C_8H + 12-H wag
	959	10-H + 12-H wag
	967	HC_7═C_8H + 11-H wag
	1000	9-Me rock
	1034	12-H + 14-H wag, 13-Me rock
	1152	C_{10}−C_{11} str
	1155	C_{10}−C_{11} str, 9-Me rock
	1200	C_8−C_9 str
	1210	C_{14}−C_{15} str
	1247	nl
	1647	C═NH str (C═ND str: 1627)

[a] Designations used in this table are as follows: Me, methyl group; wag, wagging mode; str, stretching mode; rock, rocking mode; nd, not determined; nl, not localized.

DISCUSSION

In the present study, we systematically incorporated isotope-labeled retinals into the apoprotein of iodopsin and measured the FTIR spectra of those iodopsin samples. From the spectra, the bands were assigned to specific vibrational modes (Table 1) and the results were compared to those from the resonance Raman spectra of bovine rhodopsin (*23*, *39*). The similarity and/or difference in chromophore structure between iodopsin and rhodopsin are discussed mainly in view of the chloride effect present in iodopsin.

Assignment of the C═C and C−C Stretching Modes. The ethylenic stretching mode (C═C stretching mode) of the polyene chain is observed as the largest band in the vibrational spectrum. It is generally difficult to divide each of the C═C stretching modes because of the quite effective conjugation of π-electrons and vibrational coupling. This property holds for bathoiodopsin, where the band indicated is just slightly downshifted upon labeling a carbon atom at any position of the polyene chain. On the other hand, iodopsin and isoiodopsin exhibited large band shifts upon labeling at some carbon atoms in the polyene chain. Large band splits are observed when the C_{11}═C_{12} carbons are labeled in iodopsin (Figure 3). This result implies a correlation of the cis configuration with the coupling state of the C═C stretching modes of the chromophore. The most likely picture is that there exist two conjugated C═C stretching modes corresponding to the two parts of the chromophore divided by the cis configuration in iodopsin. The band splits observed in isoiodopsin may correlate with either the cis-configuration of the chromophore or the presence of methyl groups at positions 9 and 13.

Table 2: Comparison of Band Assignments between FTIR and Resonance Raman Spectra for the Fingerprint Region.

product	mode	FTIR (cm^{-1})[a]	Raman (cm^{-1})[b]
iod	C_8−C_9 str	1219	1214
	C_{10}−C_{11} str	nd[c]	1105
	C_{12}−C_{13} str	1219, 1205	1235
	C_{14}−C_{15} str	1205	1189
batho	C_8−C_9 str	1203	1212
	C_{10}−C_{11} str	1171	1180
	C_{12}−C_{13} str	nl[d]	1232
	C_{14}−C_{15} str	1219	1212
iso	C_8−C_9 str	1200	1205
	C_{10}−C_{11} str	1152, 1155	1154
	C_{12}−C_{13} str	nl[d]	1246
	C_{14}−C_{15} str	1210	1205

[a] The present study. [b] Reference *33*. [c] Not determined. [d] Not localized.

The C−C stretching (fingerprint) vibrational modes of iodopsin, bathoiodopsin and isoiodopsin are partially assigned as summarized in Table 1 from the spectra shown in Figure 6. The C−C stretching modes have also been assigned in the resonance Raman spectrum, on the basis of analogy with that of bovine rhodopsin, as summarized in Table 2 (*33*). The conclusions of these two studies differ in the assignment of the C_{12}−C_{13} stretching mode. The C_{12}−C_{13} stretching mode is assigned to be included in the 1219 and 1205 cm^{-1} bands in the present study, while it is assigned to the 1235 cm^{-1} band in the resonance Raman study. In addition, Raman bands at 1232 and 1246 cm^{-1} of bathoiodopsin and isoiodopsin are assigned to the C_{12}−C_{13} stretching mode of the chromophore. In the FTIR difference spectra, the corresponding bands are observed at 1233, 1232, and 1247 cm^{-1} in iodopsin, bathoiodopsin, and isoiodopsin, respectively (Figure 6). In the present study, these bands are affected largely by labeling at positions other than C_{12}−C_{13}, though they are also affected by labeling at C_{12} and C_{13}. Thus, it seems to be more reasonable to assign these bands to some mixed C−C stretching mode mainly composed of modes other than the C_{12}−C_{13} stretching vibration. This result is also quite different from that of rhodopsin (*38*). The uncertainty of the C_{12}−C_{13} stretching vibration in iodopsin may reflect the more delocalized π-electrons of the chromophore than in rhodopsin, especially around the C_{12}−C_{13} region. Assignments of other C−C stretching modes are basically reasonable with slight differences in frequency, supporting the previous assignments in the resonance Raman spectrum.

Chloride Effect on the 829 cm^{-1} Mode of Bathoiodopsin. Iodopsin belongs to group L, which includes the most long wavelength-shifted visual pigments among the four groups of visual pigments usually found in cones (group S, M_1, M_2, and L). The absorption spectra of most group L pigments show a red shift upon chloride binding. In our previous studies, we investigated the effect of the anion on the chromophore structures of iodopsin and bathoiodopsin by means of low-temperature FTIR spectroscopy (*21*, *22*). We found that removal of chloride significantly affected the

HOOP bands of bathoiodopsin but not those of the original iodopsin, while the FTIR spectra of nitrate-bound iodopsin and bathoiodopsin were similar to those of anion-unbound forms. The most prominent effect of the removal of chloride was a large decrease in the intensity of the 829 cm^{-1} band of bathoiodopsin (see Figure 2 in the present study). We assigned this 829 cm^{-1} band to the 14-HOOP of the chromophore, because this band vanished in the batho/iod spectrum of 14-D-labeled iodopsin sample (*22*). In the present study, we showed that the 829 cm^{-1} band of chloride-bound bathoiodopsin was affected by ^{13}C labeling at C_{12} and C_{19} (carbon of the 9-methyl group) and by D labeling at 10, 11, 12, 14, and 15; the effect of labeling 14-D was the greatest (Figures 4 and 5). These results suggest that the 829 cm^{-1} band should be assigned to some coupled mode rather than an isolated 14-HOOP mode, because it was affected by ^{13}C labeling at C_{12} in addition to D labeling at 12 but was not affected by ^{13}C labeling at C_{14}. In the resonance Raman spectrum of bathorhodopsin, the 14-HOOP mode appears at 850 cm^{-1}, and the 12-HOOP mode appears at 858 cm^{-1} as a coupled band with the 7-, 8-, and 10-HOOP modes. The normal-mode analysis with the QCFF/PI Hamiltonian suggests that the vibrational mode assigned to the 12-HOOP significantly contains a displacement of 14-H, while the 14-HOOP mode contains little of the displacement of 12-H (*23*). Thus, the 829 cm^{-1} band of bathoiodopsin should correspond to the 858 cm^{-1} band of bathorhodopsin. The 829 cm^{-1} band of bathoiodopsin in the present FTIR spectrum corresponds to the 832 cm^{-1} band in the Raman spectrum, which is the most intense band in the region below 1000 cm^{-1} (*33*). Because, the intense HOOP mode comes from a distorted structure at the corresponding position of the chromophore (*39*), the 829 cm^{-1} mode of the bathoiodopsin could increase its intensity with distortion at C_{12} and/or C_{14}. Taken together, these results strongly suggest that, when the chloride-bound iodopsin converts to its batho intermediate, the chromophore is twisted around C_{12} to C_{14} as well as C_{11}. The behavior of the 908 cm^{-1} band, which shifts downward upon 14-D labeling, upon anion exchange or removal, also supports the idea that chloride affects the structure around the C_{14} of the chromophore of bathoiodopsin.

The 11-HOOP Mode of Bathoiodopsin. The 11- and 12-HOOP modes are observed as a coupled mode in rhodopsin, each of which appears as an isolated band in bathorhodopsin (*23*). In the case of iodopsin, the corresponding bands are observed at 974 and 960 cm^{-1} for iodopsin and at 908 and 903 cm^{-1} for bathoiodopsin. In the present study, the 974 and 960 cm^{-1} bands in iodopsin were confirmed to be coupled $HC_{11}{=}C_{12}H$ wagging modes. Simultaneously, the 908 and 903 cm^{-1} bands in bathoiodopsin are confirmed to be almost isolated 11-H wagging modes. The intense 11-HOOP band represents a twisted structure around C_{11} of the chromophore of bathorhodopsin (*39*). Thus, it is suggested that the structural change in the chromophore upon the formation of bathoiodopsin is basically similar to the change that occurs in forming bathorhodopsin, though the detailed structures of the two photoproducts are almost certainly different, as described below.

In the Raman spectrum of chloride-bound iodopsin (*33*), the 11-HOOP mode is observed at 913 cm^{-1}, though its intensity is quite small compared to other bands in the region below 1000 cm^{-1}. A similar tendency is also observed in the FTIR difference spectrum, that is, the intensities of the 11-HOOP bands are relatively small compared to other HOOP bands, especially the 829 cm^{-1} band. Thus, it is suggested in the case of bathoiodopsin that the chromophore is more twisted around the C_{12} to C_{14} region and that the C_{11} region is in a rather flat structure compared to that of bathorhodopsin. This chromophore structure may be one of the causes of the thermal reverse reaction of bathoiodopsin (see below). In addition, two additional bands are observed at 941 and 934 cm^{-1} in bathoiodopsin, which are assigned in the present study to a coupled $HC_{11}{=}C_{12}H$ wagging mode. The existence of these bands becomes clearer upon removal of chloride, where they increase in intensity, comparable to the 908 and 903 cm^{-1} peaks (Figure 2) (*21*). A corresponding mode is not observed in bathorhodopsin (*23*). Thus, the coupling between the 11- and 12-HOOP modes seems to be preserved in bathoiodopsin, in contrast to the case of bathorhodopsin. Though it is not clear why these bands increase in intensity upon removal of chloride, the results described above suggest that the geometry around the $C_{11}{=}C_{12}$ region of bathoiodopsin chromophore is somewhat different from that of bathorhodopsin and that chloride affects that geometry in addition to the C_{12} to C_{14} region. In the case of gecko green (P521) which also belongs to group L of cone pigments, removal of chloride increases the ratio of BSI (the blue-shifted intermediate) in the equilibrium between batho and BSI, where the apparent generation rate of the lumi intermediate becomes faster. In addition, the decay rate of the lumi intermediate also becomes faster upon removal of chloride (*42*). Thus, it is reasonable to assume that the chromophore of anion-free bathoiodopsin has a rather relaxed structure around $C_{11}{=}C_{12}$ compared to that of chloride-bound bathoiodopsin. The 11-HOOP vibration of bathorhodopsin is observed as an isolated mode in the Raman spectrum, while it appears as a coupled mode with the 12-HOOP in rhodopsin (*23*, *35*, *39*). We suggest that the uncoupling of the 11-HOOP mode in bathorhodopsin occurs because of a large downshift of the 12-HOOP mode that could be brought about by a nearby point charge (*23*, *35*, *39*). According to the 3D structure of bovine rhodopsin recently reported (*40*, *41*), two acidic residues (Glu 113 and Glu 181) are in the proximity of C_{12} of the chromophore. However, cis−trans isomerization would pull the hydrogen of C_{12} away from both of these Glu residues, assuming that the $C_{11}{=}C_{12}$ bond rotates toward its twisting direction (*43*). Thus, the mechanism of isolation of the 11-HOOP mode described above is unlikely. We also suggest that the coupling could be collapsed simply by twisting the $C_{11}{=}C_{12}$ bond (*23*, *35*, *39*). Assuming that this mechanism is true, the partial preservation of the $HC_{11}{=}C_{12}H$ HOOP mode in bathoiodopsin should be attributed to partial planarity of the $C_{11}{=}C_{12}$ bond of the chromophore, which is different from bathorhodopsin.

Assignment of C=N Stretching Mode of the PSB. The interaction between the protonated Schiff base (PSB) and its counterion affects the spectral properties of the visual pigment (*44*). A strong interaction between the PSB and its counterion localizes the positive charge of the chromophore, thus its spectrum shifts to short wavelengths. The environment around the PSB can be monitored by the C=N stretching vibration which couples with an N−H in-plane rocking mode (C=NH stretching mode). Because hydrogen

bonding of the N−H bond affects the N−H rocking mode of the PSB, the strength of the hydrogen bonding of PSB can be monitored by the value of the downshift in the frequency of the C=N stretching mode upon substitution of the N−H proton with deuterium: stronger hydrogen bonding produces a larger downshift (*32*, *33*). In the present study, the FTIR difference spectra of 15-^{13}C and 15-D-labeled iodopsin directly confirmed the previous assignment of the C=NH stretching mode determined on the basis of H−D exchange of the PSB proton (*22*). The effect of 15-D labeling is consistent with the previous results for bovine rhodopsin which showed that the C_{15}-H in-plane rocking mode couples with the C=NH stretching vibration (*35*−*37*). The C=NH/C=ND frequencies for iodopsin and bathoiodopsin are 1640/1618 and 1638/1614 cm^{-1}, respectively (Figure 7). These values are consistent with the results of the resonance Raman spectroscopy (*33*). In addition, the C=NH/C=ND values for isoiodopsin are determined to be 1647/1627 cm^{-1}. Thus, the values of downshift upon H−D exchange (H−D shift) for iodopsin, bathoiodopsin, and isoiodopsin are calculated to be 22, 24, and 20 cm^{-1}, respectively. The present result shows good agreement with the resonance Raman result, though the downshift is somewhat larger for bathoiodopsin in the present study (C=NH and C=ND modes of bathoiodopsin in the resonance Raman spectrum are 1638 and 1617 cm^{-1}, respectively) (*33*). This tendency is quite similar to that of rhodopsin; that is, the values of the H−D shift are almost the same between the batho state (30 cm^{-1}) and the original state (32 cm^{-1}) (*45*). These results suggest that the structural change around the PSB of the chromophore upon batho formation is basically the same for iodopsin and rhodopsin. The difference in the values of the H−D shift between iodopsin and rhodopsin may reflect the difference in the strength of the H-bonding of the PSB. The C=ND stretching mode represents its intrinsic C=N stretching mode that is affected by the delocalization of the conjugated π-electron system, while the H−D shift represents the strength between the N−H bond of C=NH and its counterion (*33*). The present result shows a good correlation between the frequency of the C=ND stretching mode and the absorption maximum, while the H−D shift has no such tendency. Thus, we suggest that the color difference between iodopsin and its photoproducts produced at −196 °C is determined by some other factor such as a position change of point charges or polar groups relative to the chromophore, rather than interaction between the PSB and its counterion.

Mechanism of the Thermal Reversion of Bathoiodopsin Back to Iodopsin. Bathoiodopsin produced at −196 °C reverts to the original iodopsin upon warming, which is different from the case of rhodopsin (*20*). This property is also affected by the anion: upon warming nitrate-bound bathoiodopsin produced at −196 °C, it decay normally, like bathorhodopsin (*19*). In addition, we found in an earlier study that the thermal reversion of anion-unbound bathoiodopsin (batho·na) is also affected by its environment. That is, thermal reversion is observed when batho·na is solubilized with detergent, while the normal decay process is observed when the sample is incorporated into liposomes (*17*, *18*). These results also suggested that the thermal reversion of the liposome sample is correlated well with the chromophore structure of bathoiodopsin which we investigated previously (*21*, *22*). In particular, the most prominent difference observed is whether the intense 829 cm^{-1} band exists (see Figure 2 in the present study). On the basis of the FTIR spectrum of 14-D-labeled iodopsin and its photoproduct at −196 °C, this 829 cm^{-1} band is assigned to the 14-HOOP mode of the chromophore (*22*). Thus, we proposed a model of the thermal reversion in which the torsion around C_{14} disturbs the relaxation of the torsion around C_{11} of the bathoiodopsin chromophore, so that the distorted all-trans chromophore is thermally isomerized to the 11-cis form (*18*). In the present study, the 829 cm^{-1} band is shown to contain the displacements of C_{12} and 12-H atoms, in addition to that of 14-H (Figures 4 and 5). Thus, this 829 cm^{-1} band could not be assigned to an isolated 14-HOOP but to some mixed mode including 14-HOOP and 12-HOOP. A corresponding band is observed at 832 cm^{-1} in the resonance Raman spectrum of chloride-bound bathoiodopsin as the most intense HOOP band (*33*). The intense HOOP band in the resonance Raman spectrum represents a twisted structure around a specific part of the chromophore (*39*). Thus, the additional torsion in the all-trans chromophore of bathoiodopsin resides around C_{12} to C_{14}, which would hinder the relaxation of the torsion at C_{11} and result in a trans-cis thermal isomerization. As has been described, Glu 181 of bovine rhodopsin, which corresponds to the chloride-binding His residue site (His194 in iodopsin) on the portion of the polypeptide linking helices III and IV, resides quite close to the chromophore. Thus, the chloride bound to His194 of bathoiodopsin could sterically affect the structure around C_{12} to C_{14} of the chromophore directly or through some residues that can interact directly with both the chromophore and the chloride. Further studies using site-specific mutants and/or retinal analogues would lead us to another step in revealing the whole picture of the chloride effect on the long wavelength visual pigments of group L, including iodopsin.

ACKNOWLEDGMENT

We thank Prof. T. G. Ebrey at the University of Washington for valuable discussion and critical reading of the manuscript; Prof. R. A. Mathies for providing us information about normal mode analyses of retinal, protonated retinal Schiff base and rhodopsins; and Drs. A. Terakita and Y. Furutani for helpful discussions.

REFERENCES

1. Wald, G., Brown, P. K., and Smith, P. H. (1955) Iodopsin, *J. Gen. Physiol. 38*, 623−81.
2. Kuwata, O., Imamoto, Y., Okano, T., Kokame, K., Kojima, D., Matsumoto, H., Morodome, A., Fukada, Y., Shichida, Y., Yasuda, K., Shimura, Y., and Yoshizawa, T. (1990) The primary structure of iodopsin, a chicken red-sensitive cone pigment, *FEBS Lett. 272*, 128−32.
3. Okano, T., Kojima, D., Fukada, Y., Shichida, Y., and Yoshizawa, T. (1992) Primary structures of chicken cone visual pigments: vertebrate rhodopsins have evolved out of cone visual pigments, *Proc. Natl. Acad. Sci. U.S.A. 89*, 5932−6.
4. Shichida, Y., and Imai, H. (1998) Visual pigment: G-protein-coupled receptor for light signals, *Cell Mol. Life Sci. 54*, 1299−315.
5. Tokunaga, F., Iwasa, T., Miyagishi, M., and Kayada, S. (1990) Cloning of cDNA and amino acid sequence of one of chicken cone visual pigments, *Biochem. Biophys. Res. Commun. 173*, 1212−7.
6. Crescitelli, F. (1978) The chloride ionochromic response: an in situ effect, *Vision Res. 18*, 1421−2.
7. Knowles, A. (1976), *Biochem. Biophys. Res. Commun. 73*, 56−62.

8. Fager, L. Y., and Fager, R. S. (1979) Halide control of color of the chicken cone pigment iodopsin, *Exp. Eye Res. 29*, 401−8.
9. Shichida, Y., Kato, T., Sasayama, S., Fukada, Y., and Yoshizawa, T. (1990) Effects of chloride on chicken iodopsin and the chromophore transfer reactions from iodopsin to scotopsin and B-photopsin, *Biochemistry 29*, 5843−8.
10. Kleinschmidt, J., and Harosi, F. I. (1992) Anion sensitivity and spectral tuning of cone visual pigments in situ, *Proc. Natl. Acad. Sci. U.S.A. 89*, 9181−5.
11. Wang, Z., Asenjo, A. B., and Oprian, D. D. (1993) Identification of the Cl(−)-binding site in the human red and green color vision pigments, *Biochemistry 32*, 2125−30.
12. David-Gray, Z. K., Cooper, H. M., Janssen, J. W., Nevo, E., and Foster, R. G. (1999) Spectral tuning of a circadian photopigment in a subterranean 'blind' mammal (Spalax ehrenbergi), *FEBS Lett. 461*, 343−7.
13. Yokoyama, S., and Radlwimmer, F. B. (1999) The molecular genetics of red and green color vision in mammals, *Genetics 153*, 919−32.
14. Sun, H., Macke, J. P., and Nathans, J. (1997) Mechanisms of spectral tuning in the mouse green cone pigment, *Proc. Natl. Acad. Sci. U.S.A. 94*, 8860−5.
15. Radlwimmer, F. B., and Yokoyama, S. (1998) Genetic analyses of the green visual pigments of rabbit (Oryctolagus cuniculus) and rat (Rattus norvegicus), *Gene 218*, 103−9.
16. Yokoyama, S., and Radlwimmer, F. B. (1998) The "five-sites" rule and the evolution of red and green color vision in mammals, *Mol. Biol. Evol. 15*, 560−7.
17. Tachibanaki, S., Imamoto, Y., Imai, H., and Shichida, Y. (1995) Effect of chloride on the thermal reverse reaction of intermediates of iodopsin, *Biochemistry 34*, 13170−5.
18. Hirano, T., Imai, H., and Shichida, Y. (2003) Effect of anion binding on the thermal reverse reaction of bathoiodopsin: anion stabilizes two forms of iodopsin, *Biochemistry 42*, 12700−7.
19. Imamoto, Y., Kandori, H., Okano, T., Fukada, Y., Shichida, Y., and Yoshizawa, T. (1989) Effect of chloride ion on the thermal decay process of the batho intermediate of iodopsin at low temperature, *Biochemistry 28*, 9412−6.
20. Yoshizawa, T., and Wald, G. (1967) Photochemistry of Iodopsin, *Nature 214*, 566−71.
21. Hirano, T., Imai, H., Kandori, H., and Shichida, Y. (2001) Chloride effect on iodopsin studied by low-temperature visible and infrared spectroscopies, *Biochemistry 40*, 1385−92.
22. Imamoto, Y., Hirano, T., Imai, H., Kandori, H., Maeda, A., Yoshizawa, T., Groesbeek, M., Lugtenburg, J., and Shichida, Y. (1999) Effect of anion binding on iodopsin studied by low-temperature Fourier transform infrared spectroscopy, *Biochemistry 38*, 11749−54.
23. Palings, I., van den Berg, E. M., Lugtenburg, J., and Mathies, R. A. (1989) Complete assignment of the hydrogen out-of-plane wagging vibrations of bathorhodopsin: chromophore structure and energy storage in the primary photoproduct of vision, *Biochemistry 28*, 1498−507.
24. Pardoen, J. A., van den Berg, E. M. M., Winkel, C., and Lugtenburg, J. (1986) Synthesis of retinals isotopically labeled at position-11, position-12, position-14 and position-20, *Recl. Trav. Chim. Pays-Bas 105*, 92−98.
25. Broek, A. D., and Lugtenburg, J. (1982) Preparation of deuterium-labeled retinals having high deuterium content on specific positions. 10-Mono-, 11-mono-, 10,11-di-, 14,20,20,20-tetradeuteri-oretinal, *Recl. Trav. Chim. Pays-Bas 101*, 102−5.
26. Zhu, Y., Ganapathy, S., Trehan, A., Asato, A. E., and Liu, R. S. H. (1992) New geometric isomers of vitamin A. 18. FT-IR spectra of all 16 isomers of retinal, their isolation, and other spectroscopic propties, *Tetrahedron 48*, 10061−74.
27. Wada, A., Fujioka, N., Tanaka, Y., and Ito, M. (2000) A highly stereoselective synthesis of 11Z-retinal using tricarbonyliron complex, *J. Org. Chem. 65*, 2438−43.
28. Lughtenburg, J. (1985) The synthesis of 13C-labeled retinals, *Pure Appl. Chem. 57*, 753−62.
29. Imai, H., Terakita, A., Tachibanaki, S., Imamoto, Y., Yoshizawa, T., and Shichida, Y. (1997) Photochemical and biochemical properties of chicken blue-sensitive cone visual pigment, *Biochemistry 36*, 12773−9.
30. Kandori, H., and Maeda, A. (1995) FTIR spectroscopy reveals microscopic structural changes of the protein around the rhodopsin chromophore upon photoisomerization, *Biochemistry 34*, 14220−9.
31. This reference was deleted during revision.
32. Baasov, T., Friedman, N., and Sheves, M. (1987) Factors affecting the C═N stretching in protonated retinal Schiff base: a model study for bacteriorhodopsin and visual pigments, *Biochemistry 26*, 3210−7.
33. Lin, S. W., Imamoto, Y., Fukada, Y., Shichida, Y., Yoshizawa, T., and Mathies, R. A. (1994) What makes red visual pigments red? A resonance Raman microprobe study of retinal chromophore structure in iodopsin, *Biochemistry 33*, 2151−60.
34. Braiman, M., and Mathies, R. (1980) Resonance Raman evidence for an all-trans to 13-cis isomerization in the proton-pumping cycle of bacteriorhodopsin, *Biochemistry 19*, 5421−8.
35. Eyring, G., Curry, B., Broek, A., Lugtenburg, J., and Mathies, R. (1982) Assignment and interpretation of hydrogen out-of-plane vibrations in the resonance Raman spectra of rhodopsin and bathorhodopsin, *Biochemistry 21*, 384−93.
36. Bagley, K. A., Balogh-Nair, V., Croteau, A. A., Dollinger, G., Ebrey, T. G., Eisenstein, L., Hong, M. K., Nakanishi, K., and Vittitow, J. (1985) Fourier-transform infrared difference spectroscopy of rhodopsin and its photoproducts at low temperature, *Biochemistry 24*, 6055−71.
37. Deng, H., and Callender, R. H. (1987) A study of the Schiff base mode in bovine rhodopsin and bathorhodopsin, *Biochemistry 26*, 7418−26.
38. Palings, I., Pardoen, J. A., van den Berg, E., Winkel, C., Lugtenburg, J., and Mathies, R. A. (1987) Assignment of fingerprint vibrations in the resonance Raman spectra of rhodopsin, isorhodopsin, and bathorhodopsin: implications for chromophore structure and environment, *Biochemistry 26*, 2544−56.
39. Eyring, G., Curry, B., Mathies, R., Fransen, R., Palings, I., and Lugtenburg, J. (1980) Interpretation of the resonance Raman spectrum of bathorhodopsin based on visual pigment analogues, *Biochemistry 19*, 2410−8.
40. Okada, T., Fujiyoshi, Y., Silow, M., Navarro, J., Landau, E. M., and Shichida, Y. (2002) Functional role of internal water molecules in rhodopsin revealed by X-ray crystallography, *Proc. Natl. Acad. Sci. U.S.A. 99*, 5982−7.
41. Palczewski, K., Kumasaka, T., Hori, T., Behnke, C. A., Motoshima, H., Fox, B. A., Le Trong, I., Teller, D. C., Okada, T., Stenkamp, R. E., Yamamoto, M., and Miyano, M. (2000) Crystal structure of rhodopsin: A G protein-coupled receptor, *Science 289*, 739−45.
42. Lewis, J. W., Liang, J., Ebrey, T. G., Sheves, M., and Kliger, D. S. (1995) Chloride effect on the early photolysis intermediates of a gecko cone-type visual pigment, *Biochemistry 34*, 5817−23.
43. Okada, T., Ernst, O. P., Palczewski, K., and Hofmann, K. P. (2001) Activation of rhodopsin: new insights from structural and biochemical studies, *Trends Biochem. Sci. 26*, 318−24.
44. Blatz, P. E., Mohler, J. H., and Navangul, H. V. (1972) Anion-induced wavelength regulation of absorption maxima of Schiff bases of retinal, *Biochemistry 11*, 848−55.
45. Palings, I., Pardoen, J. A., van den Berg, E., Winkel, C., Lugtenburg, J., and Mathies, R. A. (1987) Assignment of fingerprint vibrations in the resonance Raman spectra of rhodopsin, isorhodopsin, and bathorhodopsin: implications for chromophore structure and environment, *Biochemistry 26*, 2544−56.

BI0517077